Generation of hyper-entanglement on polarization and energy-time based on a silicon micro-ring cavity

Jing Suo, Shuai Dong, Wei Zhang,* Yidong Huang, and Jiangde Peng

Tsinghua National Laboratory for Information Science and Technology, Department of Electronic Engineering, Tsinghua University, Beijing 100084, China
**zwei@Tsinghua.edu.cn*

Abstract: In this paper, hyper-entanglement on polarization and energy-time is generated based on a silicon micro-ring cavity. The silicon micro-ring cavity is placed in a fiber loop connected by a polarization beam splitter. Photon pairs are generated by the spontaneous four wave mixing (SFWM) in the cavity bi-directionally. The two photon states of photon pairs propagate along the two directions of the fiber loop and are superposed in the polarization beam splitter with orthogonal polarizations, leading to the polarization entanglement generation. On the other hand, the energy-time entanglement is an intrinsic property of photon pairs generated by the SFWM, which maintains in the process of the state superposition. The property of polarization entanglement is demonstrated by the two photon interferences under two non-orthogonal polarization bases. The property of energy-time entanglement is demonstrated by the Franson type interference under two non-orthogonal phase bases. The raw visibilities of all the measured interference fringes are higher than $1/\sqrt{2}$, the bench mark for violation of the Bell inequality. It indicates that silicon micro-ring cavity is a promising candidate to realize high performance hyper-entanglement generation.

OCIS codes: (270.0270) Quantum optics; (190.4390) Nonlinear optics, integrated optics; (190.4380) Nonlinear optics, four-wave mixing.

References and links

1. P. G. Kwiat, "Hyper-entangled states," J. Mod. Opt. **44**(11-12), 2173–2184 (1997).
2. S. P. Walborn, "Hyperentanglement: Breaking the communication barrier," Nat. Phys. **4**(4), 268–269 (2008).
3. J. T. Barreiro, N. K. Langford, N. A. Peters, and P. G. Kwiat, "Generation of hyperentangled photon pairs," Phys. Rev. Lett. **95**(26), 260501 (2005).
4. A. Yoshizawa, R. Kaji, and H. Tsuchida, "Generation of polarization-entangled photon pairs at 1550 nm using two PPLN waveguides," Electron. Lett. **39**(7), 621 (2003).
5. Q. Zhou, W. Zhang, J. Cheng, Y. Huang, and J. Peng, "Polarization-entangled bell states generation based on birefringence in high nonlinear microstructure fiber at 1.5 μm," Opt. Lett. **34**(18), 2706–2708 (2009).
6. K.-I. Harada, H. Takesue, H. Fukuda, T. Tsuchizawa, T. Watanabe, K. Yamada, Y. Tokura, and S.-I. Itabashi, "Frequency and polarization characteristics of correlated photon-pair generation using a silicon wire waveguide," IEEE J. Sel. Top. Quantum Electron. **16**(1), 325–331 (2010).
7. S. Dong, Q. Zhou, W. Zhang, Y. He, W. Zhang, L. You, Y. Huang, and J. Peng, "Energy-time entanglement generation in optical fibers under CW pumping," Opt. Express **22**(1), 359–368 (2014).
8. L. G. Helt, Z. Yang, M. Liscidini, and J. E. Sipe, "Spontaneous four-wave mixing in microring resonators," Opt. Lett. **35**(18), 3006–3008 (2010).
9. Y. Guo, W. Zhang, N. Lv, Q. Zhou, Y. Huang, and J. Peng, "The impact of nonlinear losses in the silicon micro-ring cavities on CW pumping correlated photon pair generation," Opt. Express **22**(3), 2620–2631 (2014).
10. D. Grassani, S. Azzini, M. Liscidini, M. Galli, M. Strain, M. Sorel, J. E. Sipe, and D. Bajoni, "Emission of time-energy entangled photon pairs from an integrated silicon ring resonator," in CLEO: 2014, OSA Technical Digest (online) (Optical Society of America, 2014), paper FTh1A.3.

#231074 - $15.00 USD Received 19 Dec 2014; revised 22 Jan 2015; accepted 2 Feb 2015; published 9 Feb 2015

11. H. Takesue, H. Fukuda, T. Tsuchizawa, T. Watanabe, K. Yamada, Y. Tokura, and S. Itabashi, "Generation of polarization entangled photon pairs using silicon wire waveguide," Opt. Express **16**(8), 5721–5727 (2008).
12. H. Takesue and K. Inoue, "Generation of polarization entangled photon pairs and violation of Bell's inequality using spontaneous four-wave mixing in fiber loop," Phys. Rev. A **70**, 031802(R) (2004).
13. Q. Zhou, W. Zhang, C. Yuan, Y. Huang, and J. Peng, "Generation of 1.5 μm discrete frequency-entangled two-photon state in polarization-maintaining fibers," Opt. Lett. **39**(7), 2109–2112 (2014).
14. X. Li, P. L. Voss, J. E. Sharping, and P. Kumar, "Optical-fiber source of polarization-entangled photons in the 1550 nm telecom band," Phys. Rev. Lett. **94**(5), 053601 (2005).
15. B. Fang, O. Cohen, and V. O. Lorenz, "Polarization-entangled photon-pair generation in commercial-grade polarization-maintaining fiber," J. Opt. Soc. Am. B **31**(2), 277–281 (2014).
16. N. Lv, W. Zhang, Y. Guo, Q. Zhou, Y. Huang, and J. Peng, "1.5 μm polarization entanglement generation based on birefringence in silicon wire waveguides," Opt. Lett. **38**(15), 2873–2876 (2013).
17. H. Takesue, K. Inoue, O. Tadanaga, Y. Nishida, and M. Asobe, "Generation of pulsed polarization-entangled photon pairs in a 1.55-μm band with a periodically poled lithium niobate waveguide and an orthogonal polarization delay circuit," Opt. Lett. **30**(3), 293–295 (2005).
18. J. Brendel, N. Gisin, W. Tittel, and H. Zbinden, "Pulsed energy-time entangled twin-photon source for quantum communication," Phys. Rev. Lett. **82**(12), 2594–2597 (1999).
19. Q. Zhang, H. Takesue, S. W. Nam, C. Langrock, X. Xie, B. Baek, M. M. Fejer, and Y. Yamamoto, "Distribution of time-energy entanglement over 100 km fiber using superconducting single-photon detectors," Opt. Express **16**(8), 5776–5781 (2008).
20. N. C. Harris, D. Grassani, A. Simbula, M. Pant, M. Galli, T. Baehr-Jones, M. Hochberg, D. Englund, D. Bajoni, and C. Galland, "An integrated source of spectrally filtered correlated photons for large scale quantum photonic systems," *arXiv:1409.8215* [quant-ph] (2014)
21. N. Matsuda, P. Karkus, H. Nishi, T. Tsuchizawa, W. J. Munro, H. Takesue, and K. Yamada, "On-chip generation and demultiplexing of quantum correlated photons using a silicon-silica monolithic photonic integration platform," Opt. Express **22**(19), 22831–22840 (2014).

1. Introduction

Entangled photon pairs are important resources in quantum technologies such as quantum communication, quantum computation and quantum metrology. When a pair of photons possesses quantum entanglements on more than one degree of freedom, hyper-entanglement happens. Hyper-entangled photon pairs can carry more information, promising in many quantum information applications such as quantum dense coding and quantum key distribution [1–3].

Entangled photon pairs can be generated in nonlinear crystals through spontaneous parametric down conversion [4] or in optical fibers and silicon wire waveguides through spontaneous four wave mixing (SFWM) [5,6]. In SFWM processes, two pump photons annihilate and a pair of photons is generated simultaneously. The one with higher frequency is named signal photon and the one with lower frequency is named idler photon. Energy and momentum conservations are satisfied in these SFWM processes. Energy conservation leads to the relation of $\omega_s + \omega_i = 2\omega_p$, where ω_s, ω_i and ω_p are frequencies of signal, idler, and pump photons, respectively [7]. Momentum conservation requires the phase matching condition of $k_s + k_i = 2k_p$, where k_s, k_i and k_p are phase coefficients of signal, idler, and pump photons in the waveguides, respectively. In recent years, entangled photon pair generation in silicon micro-ring cavities focuses much attention. Compared with silica optical fibers, the third order nonlinear coefficients of silicon waveguides are much higher, and the field enhancement effect at resonance in the micro-ring cavities would further enhance the SFWM process in micro-ring cavities. Hence, ultra-high efficiencies of photon pair generations can be realized in a small footprint on a silicon photonic chip by the micro-ring cavity. On the other hand, since the spectrum of noise photons generated by spontaneous Raman scattering is narrow in silicon waveguides and easy to be filtered out, silicon micro-ring cavities support low noise photon pair generation under room temperature. Beside above advantages as nonlinear mediums, the fabrication of silicon micro-ring cavities is based on the standard complementary metal oxide semiconductor (COMS) process, showing great potential on realizing practical devices of quantum light sources. It has been demonstrated theoretically and experimentally that the micro-ring cavities are promising on high

#231074 - $15.00 USD Received 19 Dec 2014; revised 22 Jan 2015; accepted 2 Feb 2015; published 9 Feb 2015

performance correlated photon pair generation [8,9]. Recently, the property of energy–time entanglement in the photon pairs generated in a silicon micro-ring cavity is also demonstrated [10].

In this paper, we propose and demonstrate a scheme of hyper-entanglement generation on polarization and energy-time based on a silicon micro-ring cavity. In this scheme, the silicon micro-ring cavity is placed in a fiber loop including a polarization beam splitter (PBS), two fiber polarization controllers (FPCs) and the alignment system for the micro-ring cavity sample. In the fiber loop, the pump light is coupled to the micro-ring cavity sample at both ends by lensed fibers. FPCs are used to adjust the pump light polarization to stimulate the quasi-transverse electrical (quasi-TE) mode of the waveguide at both directions. Photon pairs are generated in the micro-ring cavity bi-directionally, and propagate along the clockwise and counterclockwise directions in the fiber loop, respectively. Then the two-photon states are superposed coherently in the PBS with orthogonal polarization directions to realize the polarization entanglement generation. Similar schemes have been used in polarization entanglement light sources based on silicon waveguides [11] and optical fibers [12–15]. We apply it to realize polarization entanglement generation in micro-ring cavities in this work. On the other hand, energy-time entanglement is an intrinsic property of the correlated photon pairs generated under continuous wave pumping. This scheme maintains the energy-time entanglement in the process of superposition. In the experiment, we verify the entanglement property on polarization and energy-time respectively. The polarization entanglement is demonstrated by the two photon interferences under two non-orthogonal polarization bases, while, the energy-time entanglement is demonstrated by the Franson type interferences under two non-orthogonal phase bases. The experiment results show that the SFWM in silicon micro-ring cavities provides a promising way to realize high quality hyper-entanglement.

2. The silicon micro-ring cavity sample and its property on photon pair generation

The micro-ring cavity used in this experiment is shown in Fig. 1. It is fabricated by standard CMOS processes (by Institute of Microelectronics, Singapore). It has a racetrack shape with a circumference of 132.5μm. The cross section of the waveguide in the micro-ring cavity is shown in Fig. 1(a). It has a deep ridge structure, with a width of 450nm, a ridge height of 160nm and a total height of 220nm. The micro-ring cavity is coupled to a straight waveguide with the same structure. The length of the straight waveguide is 3mm. Tapered waveguide structures are fabricated at both ends of the straight waveguide to extend the modal field, which is helpful to reduce the light coupling loss between the waveguide and lensed fibers.

#231074 - $15.00 USD Received 19 Dec 2014; revised 22 Jan 2015; accepted 2 Feb 2015; published 9 Feb 2015

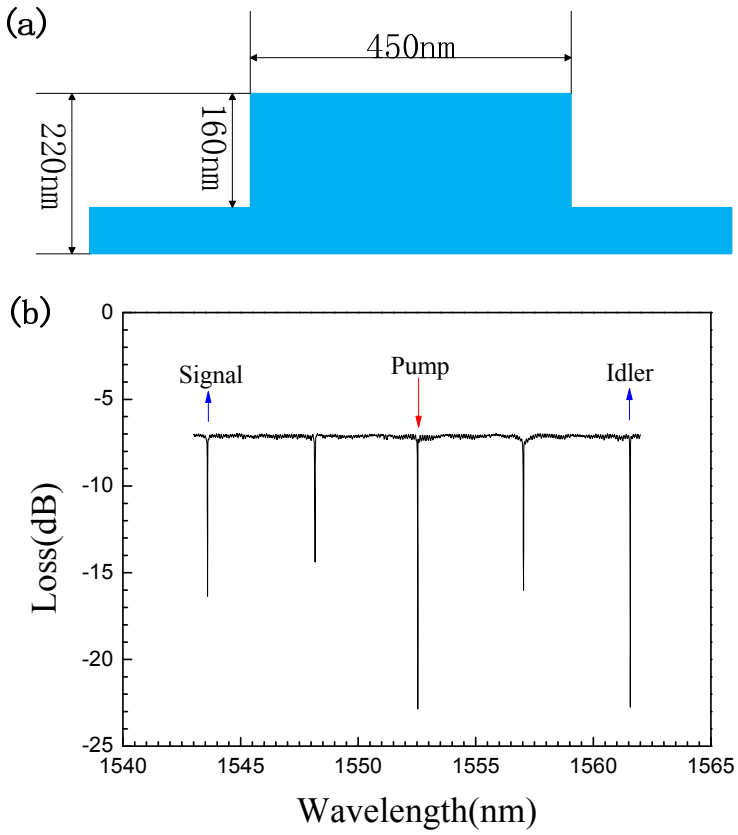

Fig. 1. The silicon micro-ring cavity sample used in the experiment. (a) Cross section of the waveguide in the micro-ring cavity. (b) Transmission spectrum of the silicon micro-ring cavity sample.

Table 1. Parameters of the resonances for the pump light and the signal / idler photons

	Resonance for signal photons	Resonance for pump light	Resonance for idler photons
Wavelength (nm)	1543.59	1552.54	1561.57
FWHM (nm)	0.012	0.01	0.016
Extinction ratio (dB)	9.5	16	15.5
Quality factor	12.86×10^4	15.5×10^4	9.76×10^4

The transmission spectrum of the micro-ring cavity sample is measured by a swept measurement system (STS-510, Santec Inc.) and shown in Fig. 1(b). The light generated from a tunable laser is coupled into and out of the straight waveguide by lensed fibers using a manual alignment system and then detected by a power meter. The dips in the spectrum indicate the resonances of the cavity, showing a free spectral range of 4.5nm at telecom band. The parameters of the selected resonances for the pump light and the signal / idler photons are shown in Table 1.

Before the experiment of hyper-entanglement generation, the property of correlated photon pair generation in the micro-ring cavity sample is measured firstly. Figure 2(a) is the setup for the measurement. The continuous wave pump light is generated by the tunable laser of the swept measurement system. After a band-pass filter module, the pump light is coupled to the micro-ring cavity sample through an alignment system with lensed fibers. A FPC is used to adjust the polarization of the pump light to stimulate the quasi-TE mode of the silicon

#231074 - $15.00 USD Received 19 Dec 2014; revised 22 Jan 2015; accepted 2 Feb 2015; published 9 Feb 2015

micro-ring cavity sample. Signal and idler photons generated in the micro-ring cavity are separated by a coarse wavelength division multiplexer (CWDM) and filtered out by tunable optical band-pass filters set at 1543.59nm and 1561.57nm, respectively. Then the signal and idler photons are detected by two free running single photon detectors (SPD1 and SPD2, Id220, IDQ Inc). The detection efficiencies and dead times of the two SPDs are set at 10% and 10μs, respectively. The single photon events detected by SPD1 and SPD2 are recorded by a time correlated single photon counter (TCSPC, DPC-230, Becker & Hickl GmbH). Figure 2(b) shows a typical measurement result of the TCSPC. The time bin width of the TCSPC is 164.6 ps. There is a coincidence count peak in the result. In the experiment, the time jitters of the two SPDs (τ_1 and τ_2) are about 400 ps under efficiencies of 10%. The coherence times of the signal and idler photons (τ_s and τ_i) are 293 ps and 220 ps, respectively, estimated by the linewidths of the resonances for the signal and idler photons. The temporal width of the coincidence count peak is estimated to be about 674 ps, agreeing with the result shown in Fig. 2(b).

Figure 2(c) shows the coincidence count to accidental coincidence count ratio (CAR) of the photon pairs generated by the silicon micro-ring cavity under different pump levels. The coincidence count is extracted from the 6 time bins covering the peak, which is indicated by the dash lines in Fig. 2(b). The accidental coincidence count is extracted from 6 time bins outside the peak. It can be seen that high quality correlated photon pair generation can be realized based on the silicon micro-ring cavity, with a maximum CAR close to 1000.

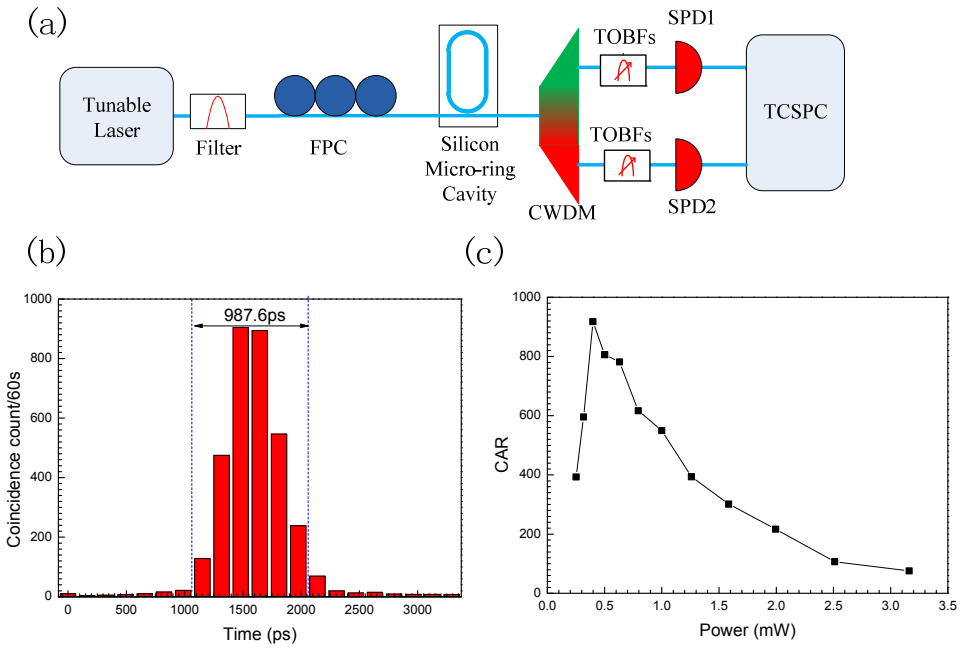

Fig. 2. The performance of correlated photon pair generation in the silicon micro-ring cavity sample. (a) Experiment setup. (b) A typical measurement result of TCSPC. (c) CAR under different pump power levels. TOBF: tunable optical band-pass filter, FPC: fiber polarization controller, CWDM: coarse wavelength division multiplexer, SPD: single photon detector, TCSPC: time correlated single photon counter.

#231074 - $15.00 USD Received 19 Dec 2014; revised 22 Jan 2015; accepted 2 Feb 2015; published 9 Feb 2015

3. The experiment of hyper-entanglement generation on polarization and energy-time based on the silicon micro-ring cavity in a fiber loop

3.1 The experiment setup and the polarization collimation process

Figure 3 shows the sketch of the experiment setup for the hyper-entanglement generation. The main part of the setup is shown in Fig. 3(a). Compared with the setup shown in Fig. 2(a), there are two modifications. Firstly, the micro-ring cavity sample is placed in a fiber loop including a polarization beam splitter (PBS), two fiber polarization controller (FPC2 and FPC3) and the alignment system. A 99:1 fiber coupler is inserted to monitor the light in the loop by power meter 2. The pump light is injected into the fiber loop through a dense wavelength division multiplexer (DWDM, ITU-31). In the fiber loop, the pump light is coupled to the micro-ring cavity sample bi-directionally by lensed fibers. FPC2 and FPC3 are used to adjust the pump light polarization to stimulate the quasi-TE mode of the waveguide at both sides. Photon pairs are generated in the micro-ring cavity and output from the fiber loop with the residual pump light. The residual pump light propagates back to the circulator through the DWDM and is detected by power meter 1 to monitor the alignment of the micro-ring cavity sample. The generated signal and idler photons are separated by the CWDM and filtered out by tunable optical band-pass filters, which are the same as the setup shown in Fig. 2(a). Secondly, to demonstrate the entanglement properties, the quantum state analyzer is required before the signal and idler photons are detected by the SPDs. The quantum state analyzer for polarization entanglement is shown in Fig. 3(b), in which the polarization states of signal and idler photons are adjusted by two fiber polarization controllers (FPC4 and FPC5) and measured by two polarizers (P1 and P2), respectively. The quantum state analyzer for energy-time entanglement is shown in Fig. 3(c), in which the signal and idler photons pass through two unbalanced Mach-Zehnder interferometers (UMZI1 and UMZI2), respectively. We used two commercial Differential Phase-Shift Keying (DPSK) demodulators (mint-1 × 2-L-2.5GHz, Kylia Inc., France) as the UMZIs. Each of them has a time difference of 400 ps between its long arm and short arm. The additional phases between the two arms of the two UMZI are denoted by α and β, which can be adjusted by applied electric voltages, respectively. The relation between the additional phase and the applied voltage in each UMZI are collimated before the experiment.

#231074 - $15.00 USD Received 19 Dec 2014; revised 22 Jan 2015; accepted 2 Feb 2015; published 9 Feb 2015

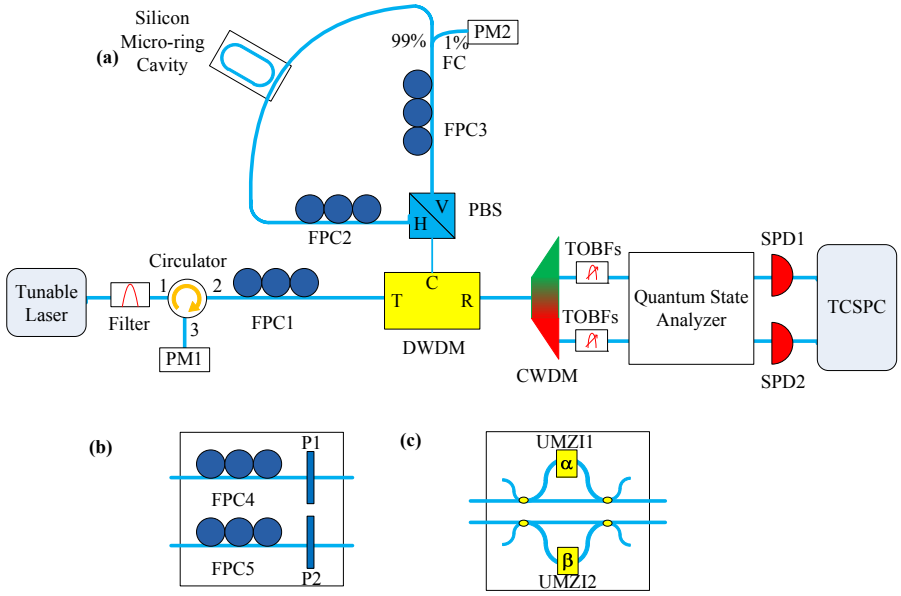

Fig. 3. Experiment setup for hyper-entanglement generation. (a) The main part. (b) The quantum state analyzer for polarization entanglement. (c) The quantum state analyzer for energy-time entanglement. PM: power meter, DWDM: dense wavelength division multiplexer, PBS: polarization beam splitter, FC: fiber coupler, P: polarizer, UMZI: unbalanced Mach-Zehnder interferometer.

To realize polarization entanglement generation in this setup, a collimation process is required to ensure that the pump light is coupled to the quasi-TE mode of the micro-ring cavity sample at both sides with equal intensity. Considering that the quantum state analyzer of polarization entanglement is placed in the setup, firstly, we adjust FPC1 to make the pump light polarized along the vertical direction of the PBS. This process can be monitored by power meter 2. Then we adjust FPC2 and FPC3 to make sure that the pump light from the vertical port of PBS is coupled to the quasi-TE mode of the micro-ring cavity sample and then output from the fiber loop through the horizontal port of the PBS. This process can be monitored by power meter 1 according to the fact that the coupling efficiency of quasi-TE mode is much better than that of the quasi-TM mode. In this status, the correlated photon pairs generated in the micro-ring cavity also output through the horizontal port of the PBS. By setting the directions of P1 and P2 to 0 rad and then adjusting FPC4 and FPC5 to realize the maximum photon count rates at both sides, the initial directions (0 rad) of P1 and P2 are collimated to the horizontal direction of the PBS. Finally, we adjust FPC1 to make the pump light split into vertical and horizontal ports of PBS equally. In this status, the pump light is coupled to the quasi-TE mode of the micro-ring cavity sample at both sides with equal intensity. The generated two photon states at both directions are coherently superposed at the PBS with orthogonal polarizations, which realizes polarization entanglement generation.

3.2 The experimental demonstration of polarization entanglement

To demonstrate the polarization entanglement of the generated photon pairs, we measure the two photon interference fringes under two non-orthogonal polarization bases. In the experiment, the pump light is set at 2dBm. The coincidence counts are recorded by TCSPC under varying directions of P1 when the directions of P2 is set at 0 rad and $\pi/4$ rad, respectively [5,16]. The count time for each record is 60 seconds, and the coincidence count is extracted from 6 time bins covering the coincidence peak. The experiment results are shown in Fig. 4. Figure 4(a) is the results of the two photon interference fringes under two

#231074 - $15.00 USD Received 19 Dec 2014; revised 22 Jan 2015; accepted 2 Feb 2015; published 9 Feb 2015

non-orthogonal polarization bases. The red solid circles and blue hollow circles are coincidence counts under varying direction of P1 when the direction of P2 is set to 0 rad and π/4 rad, respectively. The red and blue curves are their fitting curves. The raw visibilities of the fringes are 93.8 ± 2.1% and 91.3 ± 3.5% when P2 is set at 0 rad and π/4 rad, respectively. Both of them are higher than $1/\sqrt{2}$, the benchmark for violation of Bell's inequality [17]. The net visibilities of the fringes, in which the accidental coincidence counts are subtracted, are 96.4 ± 1.8% and 94.8 ± 3.6%, respectively.

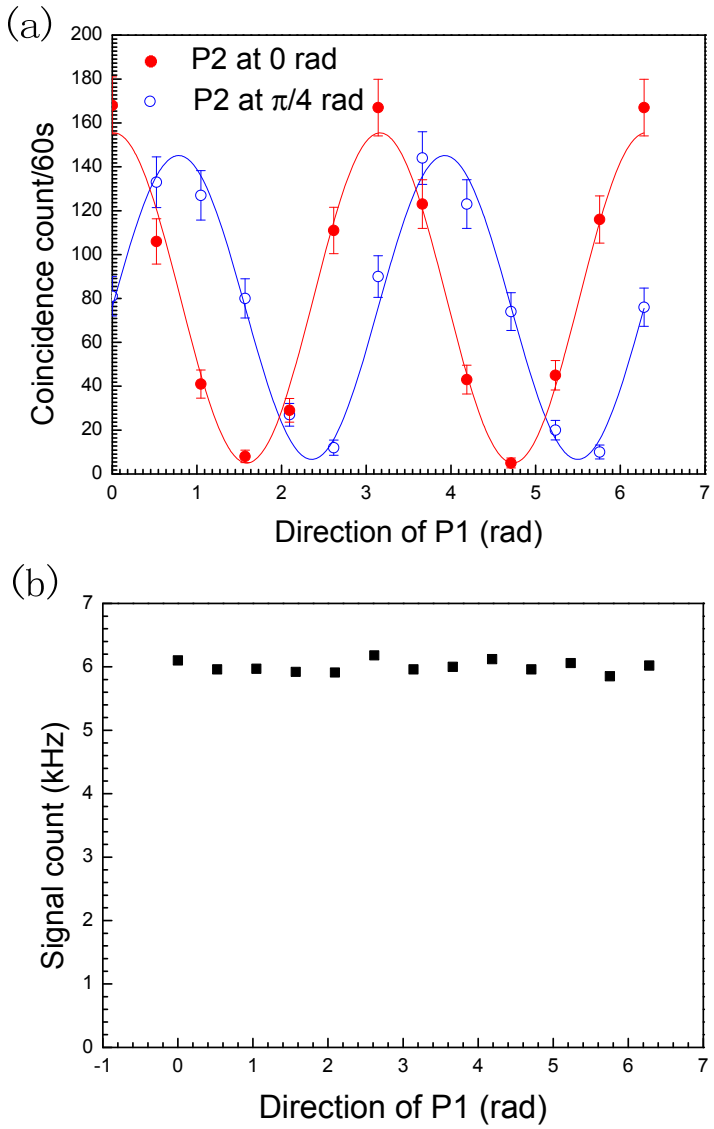

Fig. 4. Experiment demonstration of the polarization entanglement. (a) The measured two photon interference fringes under two non-orthogonal polarization bases. The red solid circles and blue hollow circles are coincidence counts under varying direction of P1 when the direction of P2 is set at 0 rad and π/4 rad respectively. The red and blue curves are their fitting curves. (b) Single side counts under varying direction of P1 when P2 is set at 0 rad.

#231074 - $15.00 USD Received 19 Dec 2014; revised 22 Jan 2015; accepted 2 Feb 2015; published 9 Feb 2015

During the measurement of the two photon interference fringes, we also record the counts of signal photons. The results are shown in Fig. 4(b). It can be seen that the signal side counts are almost unchanged as P1 changes its direction. Combining the results of two photon interferences and indistinguishability of single side count, the property of polarization entanglement in the generated photon pairs is demonstrated.

3.3 The experiment demonstration of energy-time entanglement

The quantum state analyzer shown in Fig. 2(c) is used to demonstrate the energy-time entanglement [18,19]. The time differences between two arms of the UMZIs are 400 ps. It is larger than the coherence times of the signal and idler photons. While, it is far lower than the coherence time of the two photon wave packet of the generated photon pairs, which is about 2.5μs estimated by the linewidth of the pump light. Hence, a Franson-type interference can be expected [7], which is used to demonstrate the energy-time entanglement. The experiment results are shown in Fig. 5.

Figure 5(a) shows a typical result of the coincidence counts recorded by the TCSPC using the quantum state analyzer of Fig. 3(c). In this experiment, the pump light is set at 5dBm and the detection efficiency of SPDs are set at 20%. It can be seen that there are three coincident peaks. The left and right peaks records the coincident events that one photon passes through the short arm of the corresponding UMZI while the other photon passes through the long arm of the corresponding UMZI. The central peak records the events that both signal and idler photons pass through the long arms or short arms of their corresponding UMZIs simultaneously. The two photon state of the events recorded in the central peak can be expressed as

$$\left|\Phi\right\rangle = \frac{1}{\sqrt{2}}\left(\left|s\right\rangle_{signal}\left|s\right\rangle_{idler} + e^{i(\alpha+\beta)}\left|l\right\rangle_{signal}\left|l\right\rangle_{idler}\right) \tag{1}$$

where “s” and “l” denote the short arm and long arm of the UMZIs [7]. In the experiment, we take each record in 60 seconds and extract the coincidence count from two time bins covering the central peak, which is marked between the dashed lines in Fig. 5(a).

To demonstrate the energy-time entanglement, the fringes of Franson type interference under two non-orthogonal phase bases are measured. The coincident counts of the central peak are recorded under varying α when β is set at 4.61 rad and 5.72 rad, respectively. The experiment results are shown in Fig. 5(b). The raw fringe visibilities under β = 4.61 rad and 5.72 rad are 91.6 ± 2.2% and 92.0 ± 1.3%, respectively. Both of them are higher than $1/\sqrt{2}$, the benchmark for violation of Bell’s inequality. The net visibilities of the fringes, in which the accidental coincidence counts are subtracted, are 97.2 ± 1.9% and 98.2 ± 2.8%, respectively. In the measurement, the single side count is almost unchanged under varying α regardless of β, which shows the property of indistinguishability of single side count. Hence, the energy-time entanglement of the generated pairs is demonstrated.

#231074 - $15.00 USD Received 19 Dec 2014; revised 22 Jan 2015; accepted 2 Feb 2015; published 9 Feb 2015

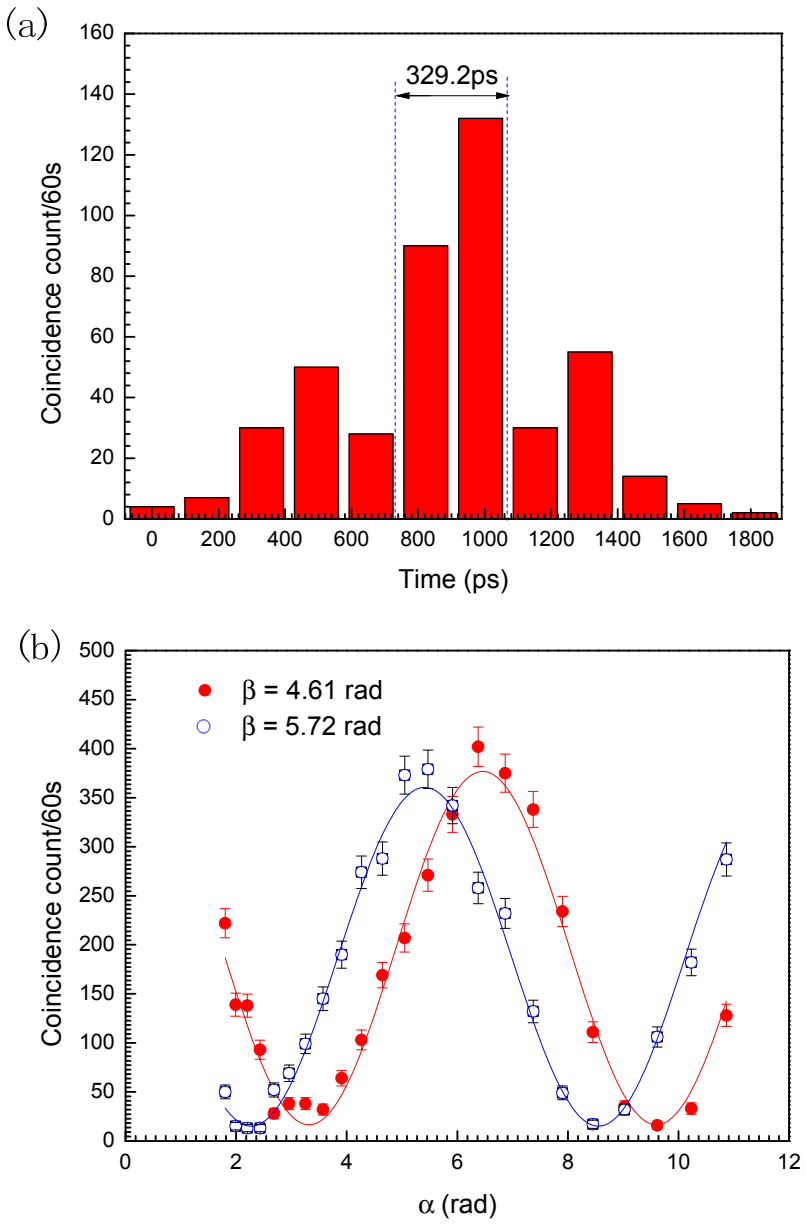

Fig. 5. Experiment demonstration of energy-time entanglement. (a) A typical result of the coincidence counts recorded by the TCSPC. (b) The measured Franson type interference fringes under two non-orthogonal phase bases. The red solid circles and blue hollow circles are coincidence counts with varying α under β = 4.61 rad and 5.72 rad, respectively.

From two experiments above, it can be seen that based on a silicon micro-ring cavity in a fiber loop, photon pairs can be generated with quantum entanglements of polarization and energy-time simultaneously, showing a property of hyper-entanglement. It is worth noting that in the experiment, the principle of the scheme is demonstrated by a setup based on fiber components. Several fiber polarization controllers are used to collimate the polarization of the

#231074 - $15.00 USD Received 19 Dec 2014; revised 22 Jan 2015; accepted 2 Feb 2015; published 9 Feb 2015

pump light and the generated photons. In recent years, silicon devices for on-chip light polarization control are developed rapidly, such as polarization rotators and polarization beam splitters [20,21]. The whole scheme has the potential to be realized on a silicon photonic chip.

4. Conclusion

In conclusion, the hyper-entanglement on polarization and energy-time is realized based on a silicon micro-ring cavity. The cavity is placed in a fiber loop connected by a polarization beam splitter. The pump light is split into two directions in the fiber loop and stimulates the SFWM processes in the cavity bi-directionally. The two photon states of the generated photon pairs in the cavity propagate along the two directions in the fiber loop and are superposed coherently with orthogonal polarizations in the polarization beam splitter, realizing the polarization entanglement generation. On the other hand, the energy-time entanglement is an intrinsic property of photon pairs generated by the SFWM and it maintains in the process of the superposition. Hence, the generated photon pairs have the property of hyper-entanglement on polarization and energy-time. The property of polarization entanglement is demonstrated by the two photon interferences under two non-orthogonal polarization bases. The raw visibilities are 93.8 ± 2.1% and 91.3 ± 3.5% when the direction of one polarization analyzer is set at 0 rad and $\pi/4$ rad, respectively. The property of energy-time entanglement is demonstrated by the Franson type interference under two non-orthogonal phase bases. The raw visibilities are 91.6 ± 2.2% and 92.0 ± 1.3% when β is set at 4.61 rad and 5.72 rad, respectively. The experiment results show that silicon micro-ring cavity is a promising candidate to realize high performance hyper-entanglement generation, which extends the applications of silicon photonic devices in the quantum information technology.

Acknowledgments

This work was supported by 973 Programs of China under Contract No. 2011CBA00303 and 2013CB328700, the National Natural Science Foundation of China under Contract No. 61307068 and 61321004, Tsinghua University Initiative Scientific Research Program under Contract No. 20131089382, and Basic Research Foundation of Tsinghua National Laboratory for Information Science and Technology (TNList).

#231074 - $15.00 USD Received 19 Dec 2014; revised 22 Jan 2015; accepted 2 Feb 2015; published 9 Feb 2015